Electronic Supplementary Material (ESI) for Journal of Materials Chemistry C.

Supporting Information

Low efficiency roll-off blue TADF OLEDs employing a novel acridine-pyrimidine based high triplet energy host

Francesco Rodella,[a] Rishabh Saxena,[b] Sergey Bagnich,[b] Dovydas Banevičius,[c] Gediminas Kreiza,[c] Stavros Athanasopoulos,[d] Saulius Juršėnas,[c] Karolis Kazlauskas,[c] Anna Köhler[b,e] and Peter Strohriegl[a,e].

[a] Macromolecular Chemistry I, University of Bayreuth, Bayreuth 95440, Germany.

[b] Soft Matter Optoelectronics, University of Bayreuth, Bayreuth 95440, Germany.

[c] Institute of Photonics and Nanotechnology, Vilnius University, Saulėtekio av. 3, LT-10257 Vilnius, Lithuania.

[d] Departamento de Física, Universidad Carlos III de Madrid, Avenida Universidad 30, 28911 Leganés, Madrid, Spain.

[e] Bayreuth Institute of Macromolecular Research (BIMF), University of Bayreuth, Bayreuth 95440, Germany.

Table of contents:

Donors and acceptors used for spectroscopic studies:

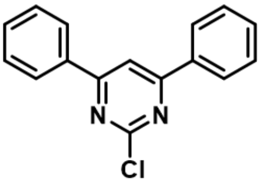

2PhPy

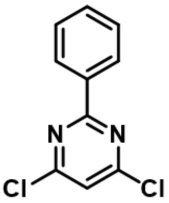

1PhPy

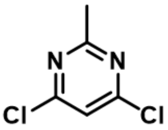

MePy

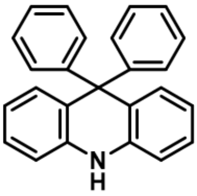

Acridine

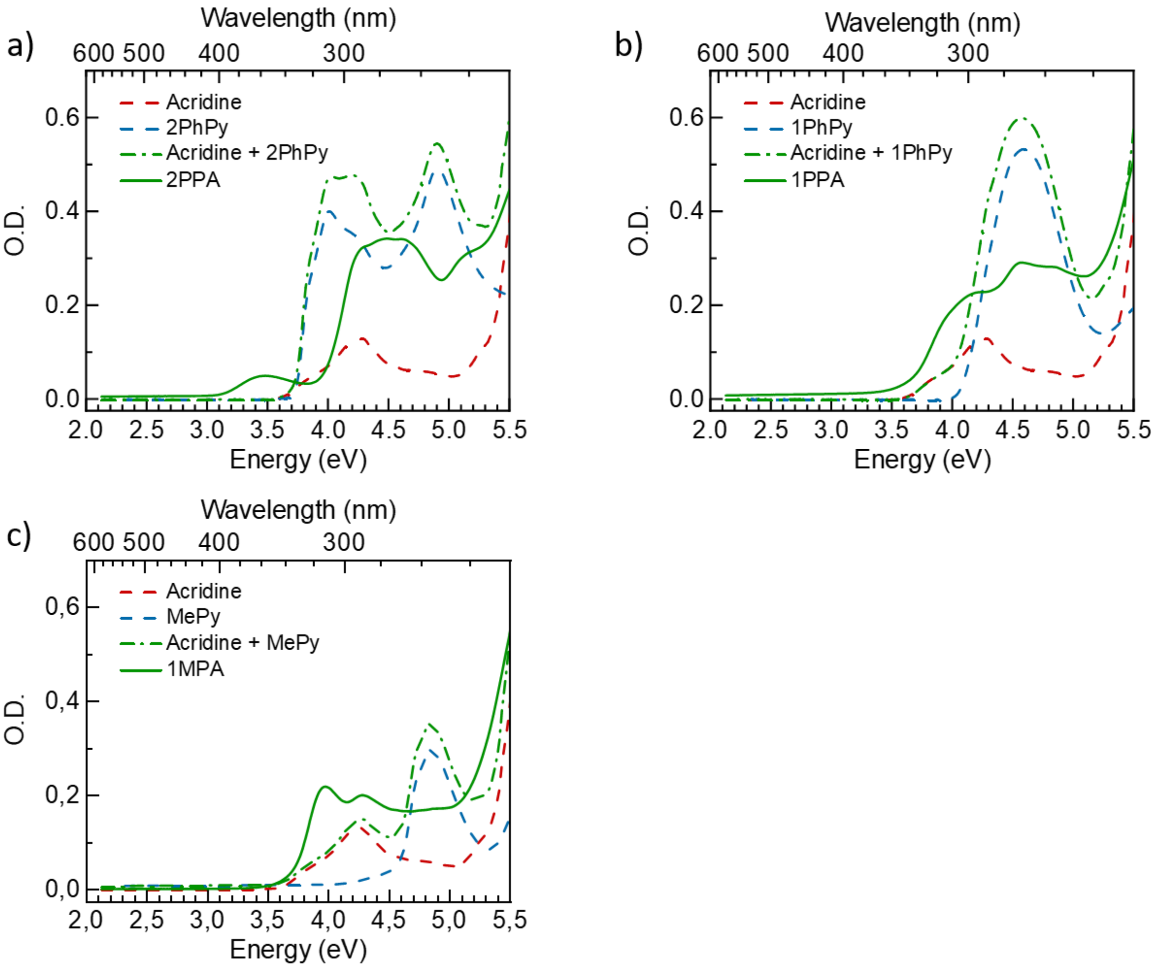

Figure S1: a), b) and c) show the absorption spectra (solid green line) of **2PPA**, **1PPA** and **1MPA** solutions (concentration = 0.05 mg/mL) in toluene along with acridine absorption (dashed red line) and **2PhPy**, **1PhPy** and **MePy** acceptors (dashed blue line) respectively. The sum of donor and acceptor absorption is shown by green dash-dot line. d) Acridine and 2PhPy (red and blue dashed line) absorption spectra in Figure S1 a are shifted in energy to match the sum of acridine + 2PhPy spectrum (green dash-dot line) with the absorption spectrum of **2PPA** (solid green line).

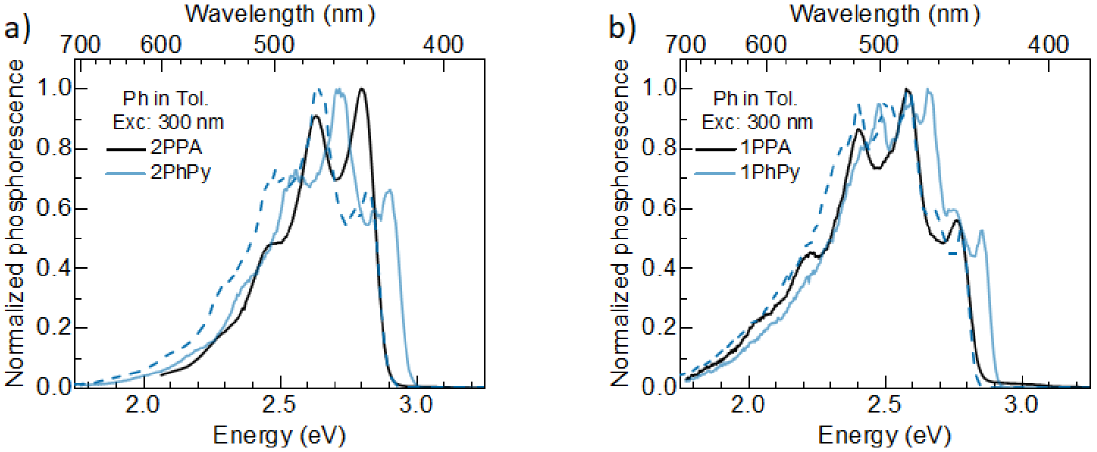

Figure S2: a) and b) show the comparison of **2PPA** and **1PPA** spectra (black line) with the horizontally translated Ph spectra of **2PhPy** and **1PhPy** spectra (blue dashed line) respectively. For reference the original **2PhPy** and **1PhPy** spectra is shown with a semi-transparent blue line.

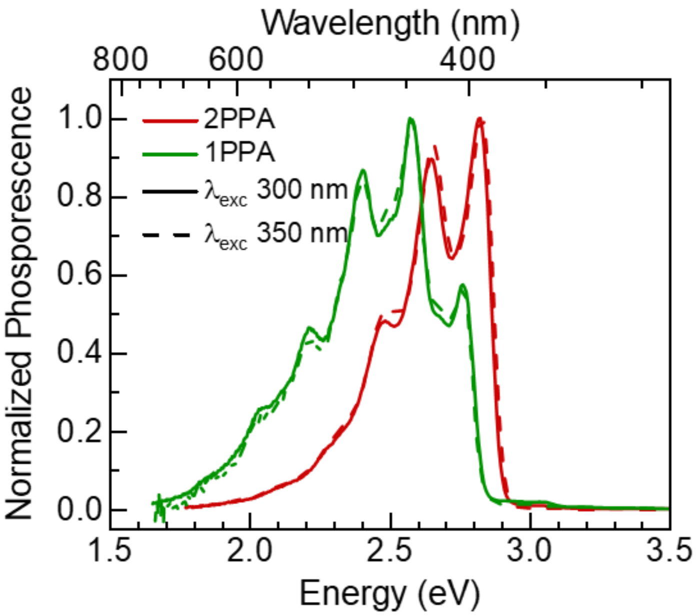

Figure S3: Excitation wavelength Ph spectra is shown for **2PPA** and **1PPA** in mTHF.

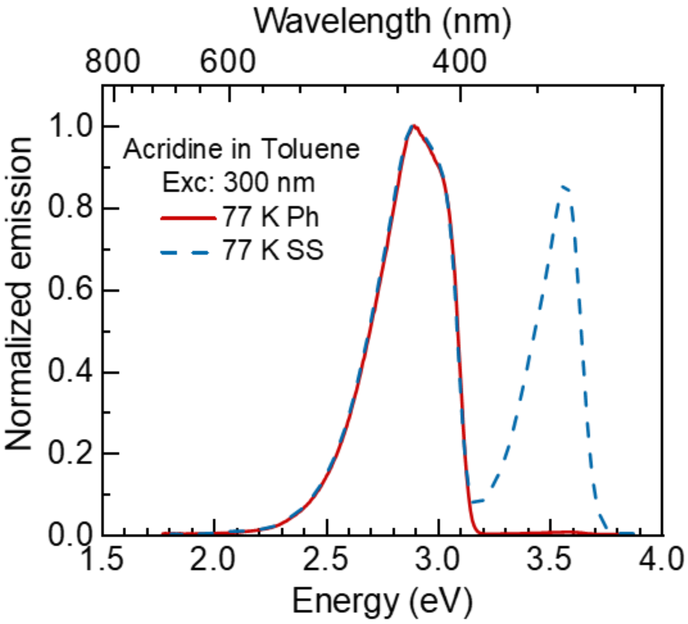

Figure S4: 77 K phosphorescence (red solid line) and steady-state (blue dashed line) for acridine solution in toluene (concentration = 0.05 mg/mL). Phosphorescence is collected with a delay time of 150 ms and a gate width of 50 ms.

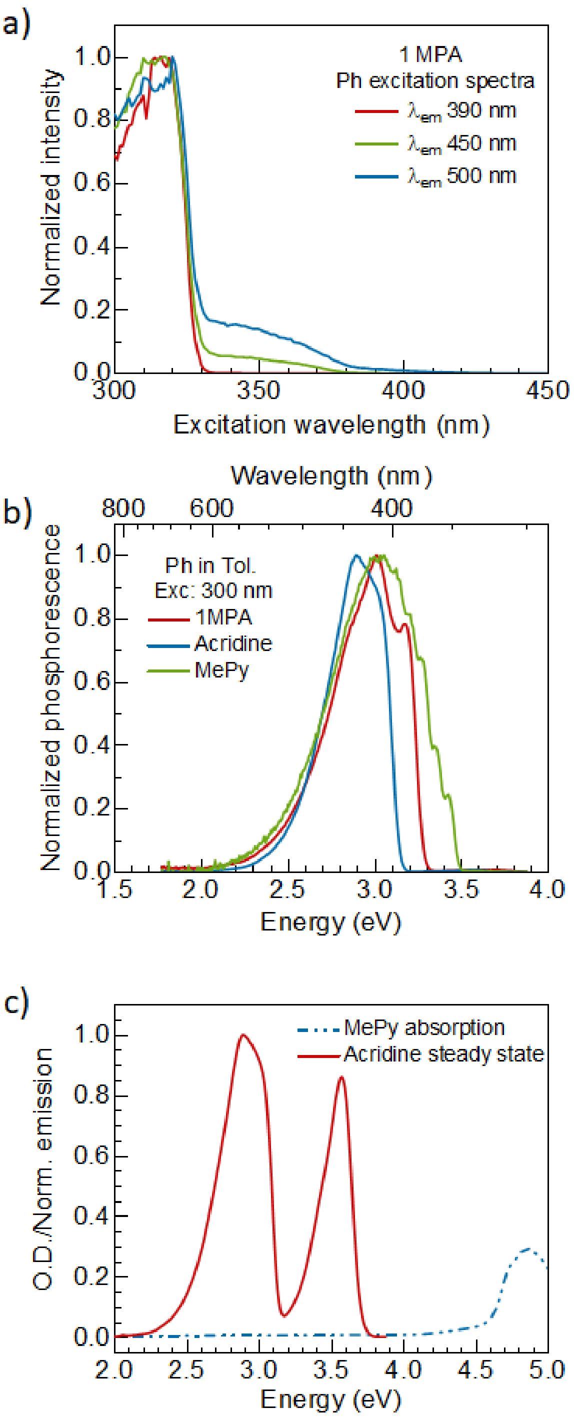

Figure S5: a) Phosphorescence (delay time 50 ms, gating time 50 ms) excitation spectrum for 1MPA solution in toluene glass (77 K). b) 77 K phosphorescence for 1MPA (red), acridine (blue) and methylpyriminine (MePy – green) solution in toluene (concentration = 0.05 mg/mL). Phosphorescence is collected with a delay time of 150 ms and a gate width of 50 ms. c) MePy absorption (blue dash-dot-dot line) and 77 K SS steady state emission of acridine solution (red solid) in toluene.

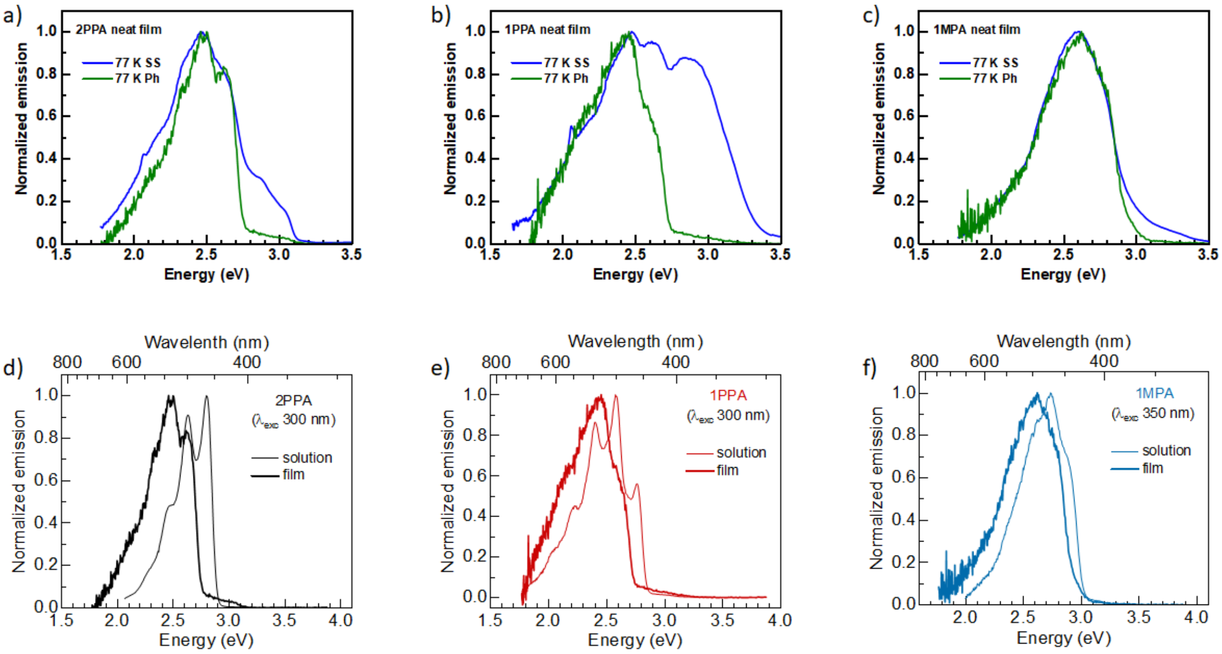

Figure S6: 77 K steady state (SS) and phosphorescence (delay time: 150 ms, gating time: 50 ms) spectra for a) 2PPA b) 1PPA and c) 1MPA neat films. 77 K phosphorescence (Ph) spectra in neat films compared with the Ph spectra in frozen toluene solution for d) 2PPA e) 1PPA and f) 1MPA.

Assignment of singlet and triplet states for 1MPA

S_2 is an acridine based locally excited (LE) state (by comparison of steady state emission of 1MPA in **Figure 3e** with the steady state emission of acridine in **Figure S4**).

Option A: High energy 1MPA phosphorescence (T_2) is acridine based phosphorescence as it is observed only when acridine is excited, i.e. when $\lambda_{exc} <$ 330 nm (**Figure S5a** and **Figure S1**). This also implies that the intersystem crossing (ISC) rate on acridine is faster and that the charge transfer (CT) from acridine to methylpyrimidine (MePy) to form a CT state is slower. The internal conversion from the high energy triplet state (T_2) to the low energy triplet state (T_1) is also slow because of the required CT.

Option B: High energy 1MPA phosphorescence (T_2) is from MePy based LE.

- **Argument in favor of it:** The MePy phosphorescence is close in energy to the observed T_2 emission (**Figure 5b**).
- **Arguments against it:** the absorption from MePy is very far away from the excitation energy ($\lambda_{exc} =$ 300 nm, $E_{exc} =$ 4.13 eV), i.e. MePy cannot be excited. Thus, the excitation would need to be transferred from acridine to MePy. However, the emission of acridine has negligible overlap with the MePy absorption (**Figure S5c**), implying poor energy transfer between these two units, since for excitations to be transferred efficiently via Förster/Dexter process some overlap is required.

Low energy 1MPA phosphorescence (T_1): It is assigned as an acridine based hybrid CT-LE state because emission at both 450 and 500 nm have strong contribution from acridine excitation ($\lambda_{exc} <$ 330 nm) in the phosphorescence excitation spectrum (**Figure 5a**). The phosphorescence spectral shape (**Figure 3f**) has some signatures of acridine phosphorescence (**Figure S4**). Also, there is some weak absorption between 330-380 nm (**Figure S5a**) consistent with the expected position of CT absorption.

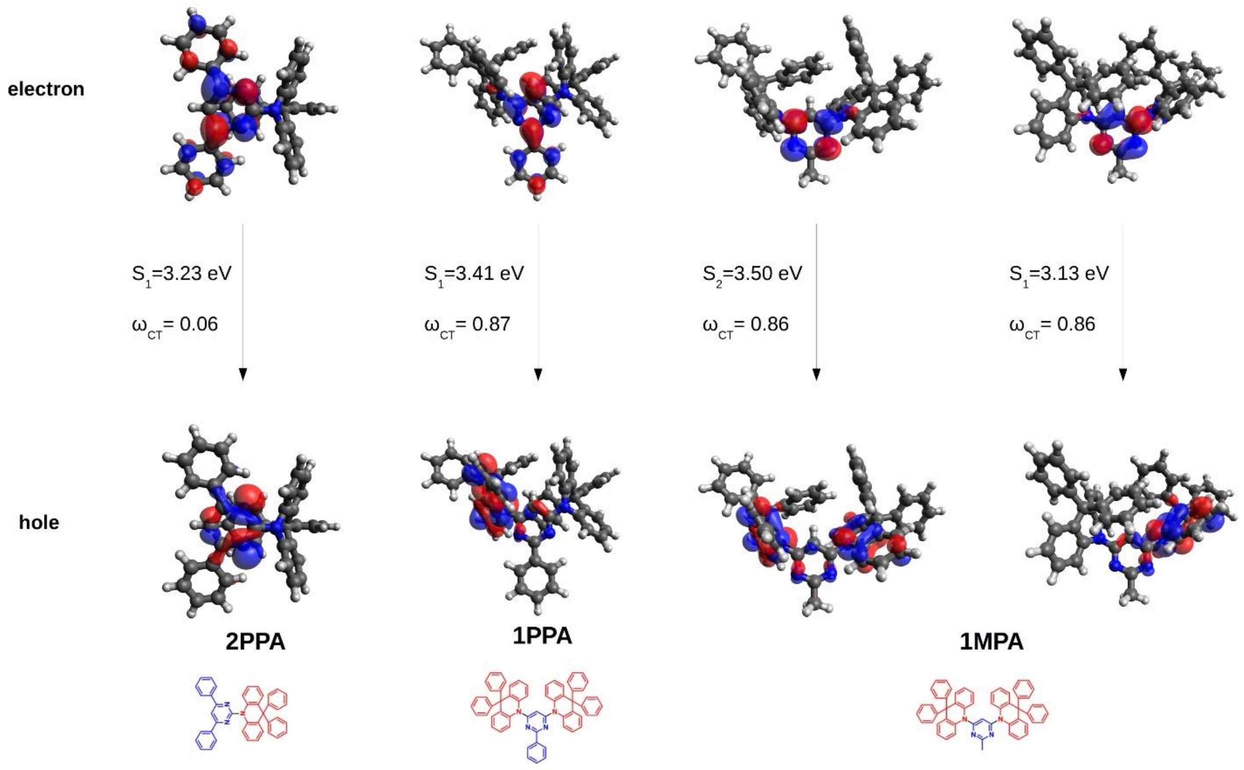

Figure S7: TDA-DFT computed natural transition orbitals, emission energies and charge transfer numbers for the lowest relaxed singlet states for **2PPA**, **1PPA** and **1MPA** at the M06-2X/6-31+G(d,p) level. For **1MPA** both the S_2 and S_1 state NTOs are shown. The relevant arrangement of the acridine and pyrimidine units is shown at the bottom.

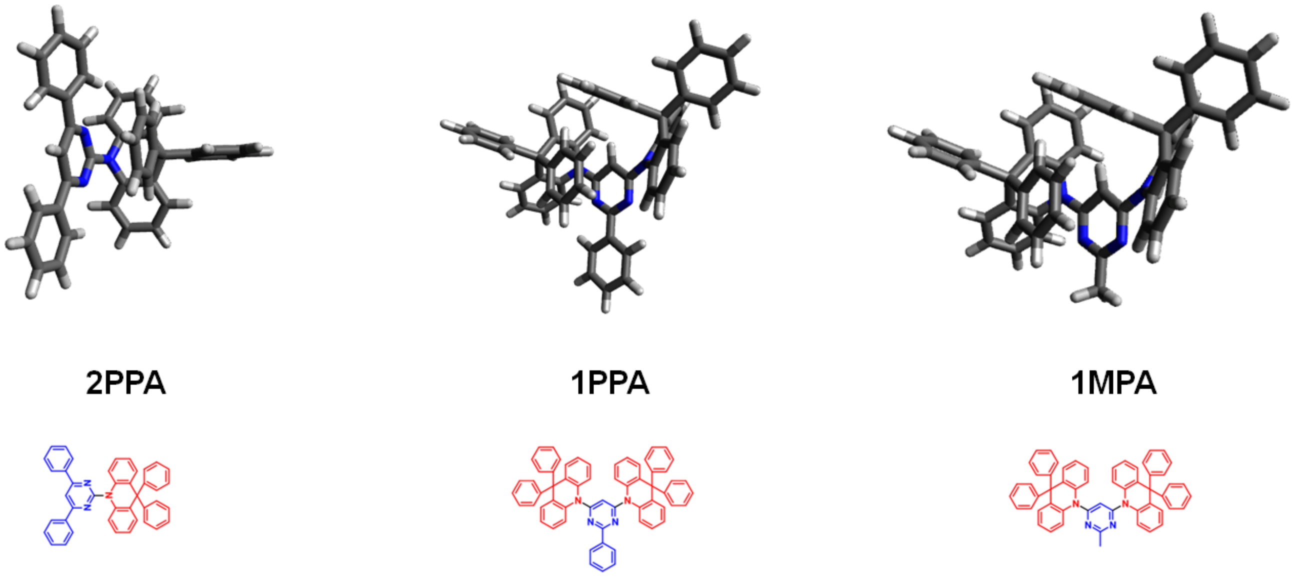

Figure S8: TDA-DFT optimized structures for the lowest triplet state for **2PPA**, **1PPA,** and **1MPA** at the M06-2X/6-31+G(d,p) level. The structures from Figure 4b (top view) of the main text are reproduced here to present a side view of the optimized triplet geometries.

Table S3: Charge transfer numbers **ω_{CT}** and average electron-hole separation distance **Δr** for the lowest relaxed singlet and triplet excited states of **1PPA** and **1MPA**.

compound/state	**ω_{CT}**	**Δr (Å)**
1PPA/S_1	0.87	4.44
1PPA/T_1	0.27	3.09
1MPA/S_2	0.86	2.07
1MPA/S_1	0.86	3.26
1MPA/T_1	0.45	1.92

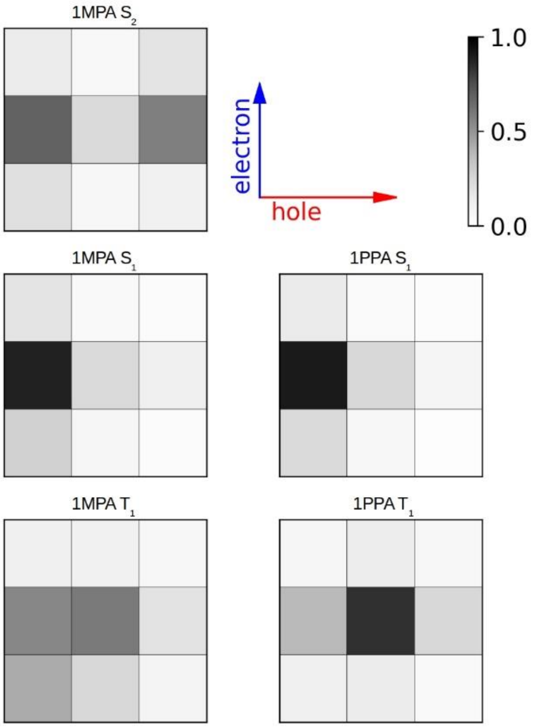

Figure S9: Electron-hole pair correlation plots of the Ω matrix with respect to the acridine-pyrimidine-acridine fragments for the lowest singlet and triplet state of **1PPA** and **1MPA.**

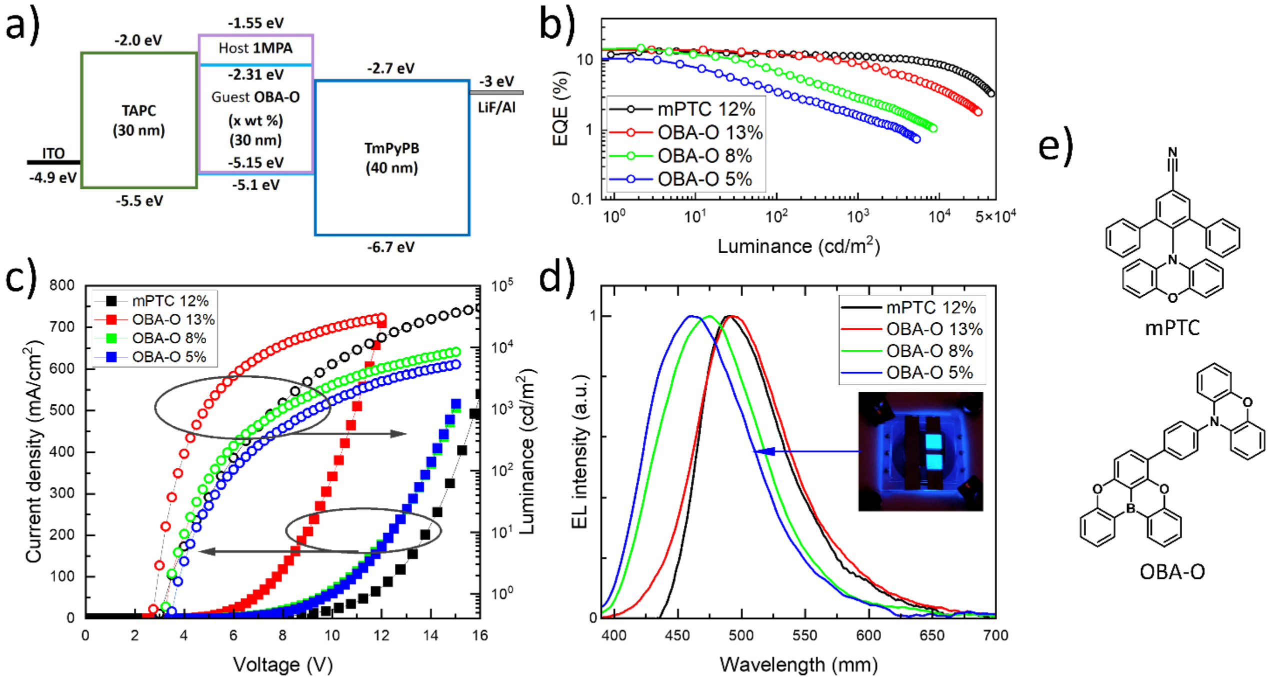

Figure S10: Main properties of the TADF OLED based on **1MPA** host doped with 5, 8 and 13 wt% of **OBA-O**. a) energy level diagram. b) EQE vs. luminance. c) current density and luminance vs. applied voltage. d) electroluminescence spectrum with working device picture shown in the inset. The properties of analogous device with **mPTC** (12 wt%) emitter is shown for reference. e) Molecular structure of the emitters.

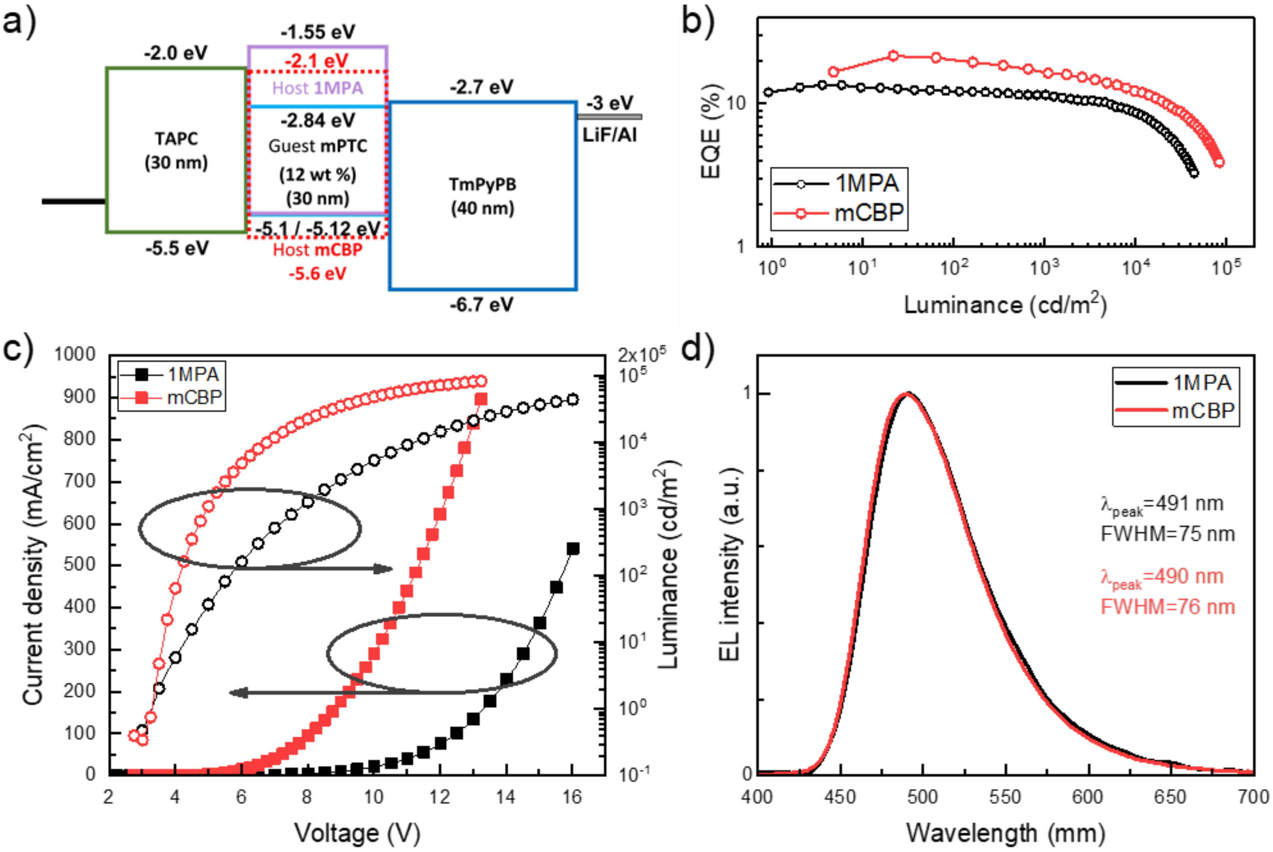

Figure S11: Comparison of the TADF OLEDs based on the new host **1MPA** vs. the benchmark host **mCBP**. Both the OLEDs have a doping concentration of 12 wt% of **mPTC**. a) energy level diagram. b) EQE vs. luminance. c) current density and luminance vs. applied voltage. d) electroluminescence spectrum.

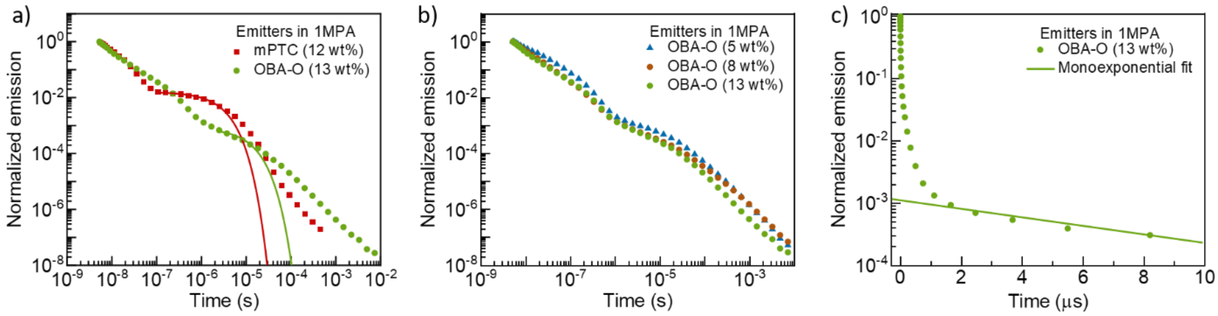

Figure S12: a) RT PL decay of **mPTC** (12 wt%) and **OBA-O** (13 wt%) doped films in **1MPA**. Also shown are monoexponential fits to the decay of the delayed component of 2μs and 9μs, respectively. b) RT PL decay of **OBA-O** (5, 8 and 13 wt%) doped films in **1MPA**. c) RT PL decay of OBA-0 in 1MPA (13 wt%) on a semilogarithmic scale, along with a monoexonential fit of 9μs lifetime.

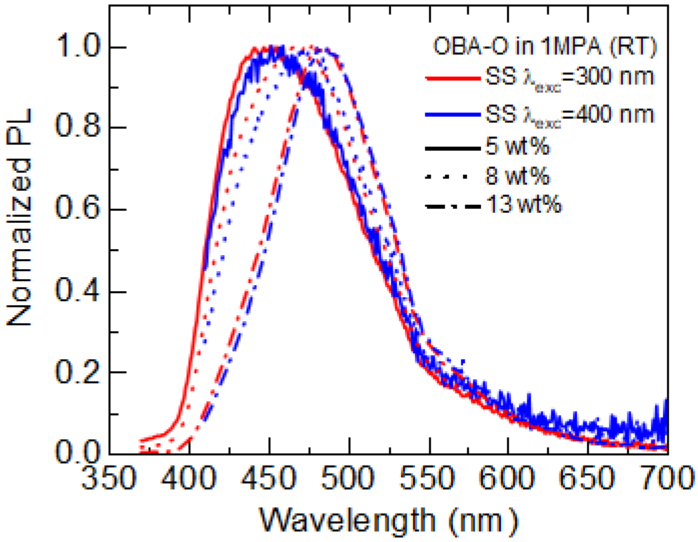

Figure S13: Room temperature photoluminescence spectra of OBA-O doped films (5, 8 and 13 wt%) in 1MPA. The spectra are shown for two excitation wavelengths: when excitons are generated only on emitter molecules (λ_{exc} = 400 nm - blue lines) and on both host and emitter (λ_{exc} = 300 nm - red lines).

Table S1: Photolominescence quantum yield measurements of mPTC and OBA-O with different doping percentage in **1MPA** host.

mPTC (wt%) in 1MPA	PLQY (%)	OBA-O (wt%) in 1MPA	PLQY (%)
5	53	5	29
10	69	10	51
12	71	20	42
20	72		

Table S2: A summary of average delayed fluorescence (DF) lifetimes for the PL decays of doped emitter films in **1MPA**.

Emitter in 1MPA	Doping concentration	Monoexponential delayed lifetime	Average delayed lifetime
mPTC	12 wt%	2 µs	6 µs
OBA-O	5 wt%	11 µs	218 µs
	8 wt%	11 µs	343 µs
	13 wt%	9 µs	191 µs

The monoexponential delayed lifetime gives the dominant contribution to the decay. In the film, there are further contributions at longer lifetimes that can arise from tail states in the DOS, triplet-triplet annihilation and phosphorescence. If these longer-lived contributions are included, an average delayed fluorescence (DF) lifetime is obtained according to $\left(\tau_{avg} = \frac{\int t.I_{DF}dt}{\int I_{DF}dt}\right)$.